CLINICAL ORTHOPAEDICS AND RELATED RESEARCH
Number 448, pp. 157–163

Rotator Cuff Muscle Architecture

Implications for Glenohumeral Stability

Samuel R. Ward, PT, PhD*; Eric R. Hentzen, MD, PhD*; Laura H. Smallwood, BS*; Robert K. Eastlack, MD*; Katherine A. Burns, MD†; Donald C. Fithian, MD†; Jan Friden, MD, PhD‡; and Richard L. Lieber, PhD*

We examined the architectural properties of the rotator cuff muscles in 10 cadaveric specimens to understand their functional design. Based on our data and previously published joint angle-muscle excursion data, sarcomere length operating ranges were modeled through all permutations in 75º medial and lateral rotation and 75º abduction at the glenohumeral joint. Based on physiologic cross-sectional area, the subscapularis would have the greatest force-producing capacity, followed by the infraspinatus, supraspinatus, and teres minor. Based on fiber length, the supraspinatus would operate over the widest range of sarcomere lengths. The supraspinatus and infraspinatus had relatively long sarcomere lengths in the anatomic position, and were under relatively high passive tensions at rest, indicating they are responsible for glenohumeral resting stability. However, the subscapularis contributed passive tension at maximum abduction and lateral rotation, indicating it plays a critical role in glenohumeral stability in the position of apprehension. These data illustrate the exquisite coupling of muscle architecture and joint mechanics, which allows the rotator cuff to produce near maximal active tensions in the midrange and produce passive tensions in the various end-range positions. During surgery relatively small changes to rotator cuff muscle length may result in relatively large changes in shoulder function.

Received: May 26, 2005
Revised: November 18, 2005; January 4, 2006
Accepted: February 7, 2006
From the *Department of Orthopaedics and Bioengineering, University of California and Veterans Administration Medical Centers, San Diego, CA; the †Department of Orthopaedic Surgery, Kaiser Permanente Medical Group, San Diego, CA; and the ‡Department of Hand Surgery, University of Göteborg and Sahlgrenska University Hospital, Göteborg, Sweden.
One or more of the authors (SRW, DCF, JF, RLL) has received funding from the Department of Veterans Affairs Rehabilitation Research and Development, the Swedish Research Foundation, the Kaiser Permanente Foundation, and NIH grants AR40050 and HD048501.
Each author certifies that his or her institution has waived approval for the human protocol for this investigation and that all investigations were conducted in conformity with ethical principles of research.
Correspondence to: Richard L. Lieber, PhD, Department of Orthopaedics (9151), V.A. Medical Center and U.C. San Diego, 3350 La Jolla Village Drive, San Diego, CA 92161. Phone: 858-552-8585, ext. 7016; Fax: 858-552-4381; E-mail: rlieber@ucsd.edu.
DOI: 10.1097/01.blo.0000194680.94882.d3

Rotator cuff muscles function dynamically to stabilize the spherical humeral head in the shallow glenoid fossa.[5] Rotator cuff tears are common, affecting approximately 7% of elderly patients.[10] These tears frequently lead to debilitating instability and pain. The supraspinatus tendon is the most commonly damaged structure in rotator cuff tears.[5,13] In small or medium-sized tears, tendon mobilization alone may permit direct repair without imposing undue tension on the reconstructed tendon.[24] However, after larger or chronic tears, the tendon and muscle belly often retract, leading to difficulty in repairing the tendon stump to its original anatomic insertion. The degree of lengthening during rotator cuff mobilization is unknown. The impact of changing the resting length of these muscles on force-generating capacity is also unknown. This is because the detailed architectural properties of the rotator cuff muscles have not been well defined.

Skeletal muscle architecture has been defined as the arrangement of muscle fibers relative to the axis of force generation.[11,16] Investigations performed across muscle groups in varied species have consistently upheld the tenet that muscle architecture provides the only anatomic basis for successful prediction of muscle force and excursion.[4,25] Gross physical parameters, such as muscle mass and volume, and metabolic parameters, such as fiber type distribution, substantially influence contractile properties. However, none predict muscle function as well as muscle architecture.[4,16,25] Force generation, contraction velocity, and excursion may be predicted accurately by analyzing the arrangement, length, and number of muscle fibers. Implementation of surgical reconstructive procedures has evolved based on the increased understanding of muscle function derived from studies of muscle architecture.[8,9,15,17]

Detailed study of the architectural design of the rotator cuff muscles can provide insight into how the glenohumeral joint is stabilized. Although the architectural characteristics of the rotator cuff have been reported,[2,3,26] these studies did not measure the length of the sarcomeres in the

muscles. This measurement is critical because the sarcomere is the basic unit of force generation, determining passive and active muscle contractile properties.[12] Previously published data are unreliable because of limited information regarding the sarcomere length at which muscle fiber length and physiologic cross-sectional area (PCSA) were calculated. The sarcomere length-joint angle relationship (operating range) is the only method for predicting relative muscle force as a function of joint angle. This measurement can predict the effects of reparative techniques and provide insight into normal muscle function.

We asked whether muscle fiber length and PCSA differed between muscles of the rotator cuff. Using that information and a model of the glenohumeral joint, we estimated the sarcomere length-joint angle relationships of each muscle to predict the contribution of each muscle to shoulder function as a function.

MATERIALS AND METHODS

Ten shoulders free of arthritis, tendon disruption, or other visible disorders were obtained from 10 fresh frozen cadavers (age, 89 ± 12 years; male to female ratio, 5:5; humeral head diameter, 4.42 cm ± 0.37 cm). Muscle architecture was determined according to the methods of Sacks and Roy[27] as previously described by Lieber et al[15] for muscles of the upper extremity. The humerus was transected just distal to the deltoid insertion and the skin and overlying muscles including the deltoid were removed. The scapula and proximal humerus were freed from the chest wall, leaving the rotator cuff muscles intact (supraspinatus, infraspinatus, subscapularis, and teres minor). Specimens were positioned in 0° abduction, 0° flexion, and 0° lateral rotation and immersed in 10% buffered formaldehyde for 72 hours. The deltoid tuberosity and humeral shaft were placed parallel and in the same plane as the vertebral border of the scapula. After fixation, the coracoid process and scapular spine were cut to expose the supraspinatus and subscapularis (Fig 1). After mapping the locations for muscle fascicle harvesting, the proximal and distal tendinous attachments of each muscle were dissected free of their bony attachments. Because the muscles had been fixed, detachment of the fascicles did not change their resting length or the resting length of the sarcomeres in them. The muscles were placed in phosphate buffered saline (PBS) for 24 to 48 hours to remove residual fixative. Specimens were removed from the buffer, gently blotted dry, and weighed.

Muscle length (L_m) was defined as the distance from the origin of the most proximal fibers to the insertion of the most distal fibers in each tendon. Surface pennation angle was measured with a standard goniometer as the angle between the fibers in each region and the distal tendon of each muscle. In subregions with well-defined tendons (eg, those in the subscapularis), pennation angles were defined as the angle between fibers in that subregion and the distal tendon for that subregion.

We carefully dissected muscle fiber bundles (fascicles) from the proximal tendon to the distal tendon of each muscle region. The bundle length was measured using a digital caliper (accuracy, 0.01 mm). The bundles were placed in mild sulfuric acid solution (15% v/v) for 30 minutes to partially digest surrounding connective tissue and then rinsed in PBS. Rotator cuff muscle fibers were sampled from predefined regions to objectively define the architectural properties and to identify region-specific architectural differences. Regions SS–A1, A2, and A3 of the supraspinatus (Fig 1A) were located on the anterior head, whereas regions SS–P1 and P2 were located on the posterior head. These two regions of supraspinatus have been described.[26,28,29] Regions 1, 2, and 3 of the infraspinatus, teres minor, and subscapularis corresponded to the superior, middle, and inferior portions (Fig 1B–C). Under magnification, three small muscle fiber bundles (consisting of approximately 20 single fibers) were isolated from each muscle region and mounted on slides. The sarcomere length (L_s) for the dissected bundles was determined by laser diffraction using the zeroth-to-first order diffraction angle.[15] Values for sarcomere number (S_n) and normalized fiber length (L_f) were calculated for the isolated bundles according to the following equations[18]:

$$Sn = \frac{L_{f'}}{L_{s'}}$$

and

$$L_f = L_{f'}\left(\frac{2.7\ \mu m}{L_{s'}}\right)$$

where *Lf'* is the measured muscle fiber length, *Ls'* is the measured sarcomere length in each fiber bundle, and *Lf* is normalized muscle fiber length. This normalization value was used because it represents the optimum sarcomere length in human muscle.

We also calculated the L_f/L_m ratio and PCSA according to the following equation[25]:

$$\text{PCSA}\ (mm^2) = \frac{M\ (g)\ g\cos\theta}{\rho(g/m^3)\ gL_f\ (mm)}$$

where θ is pennation angle and ρ is muscle density (1.112 g/cm^3).[31] The L_f/L_m ratio is an index of the excursion design. For example, if muscles contain fibers spanning the length of the muscle (L_f/L_m ratio = 1), they are designed more for excursion compared with muscle fibers spanning ½ the muscle length (L_f/L_m ratio = 0.5). This ratio is useful because it is independent of the absolute magnitude of muscle-fiber length. The PCSA is proportional to a muscle's maximum force-producing capacity.[25]

We examined how muscle fiber lengths scale with skeletal dimensions by using simple linear regression to compute the relationship between normalized muscle fiber length and the anteroposterior (AP) diameter of the humeral head. It also would have been useful to understand how the PCSA scales with body size; however, body mass was not available for any of the specimens.

We created a simple lumped parameter model to define the sarcomere length-joint angle and to determine relative tension-joint angle relationships between each muscle and the glenohumeral kinematics. The muscle architecture (resting sarcomere length, average normalized fiber length, and PCSA) was determined using our primary data. Muscle excursion-joint angle

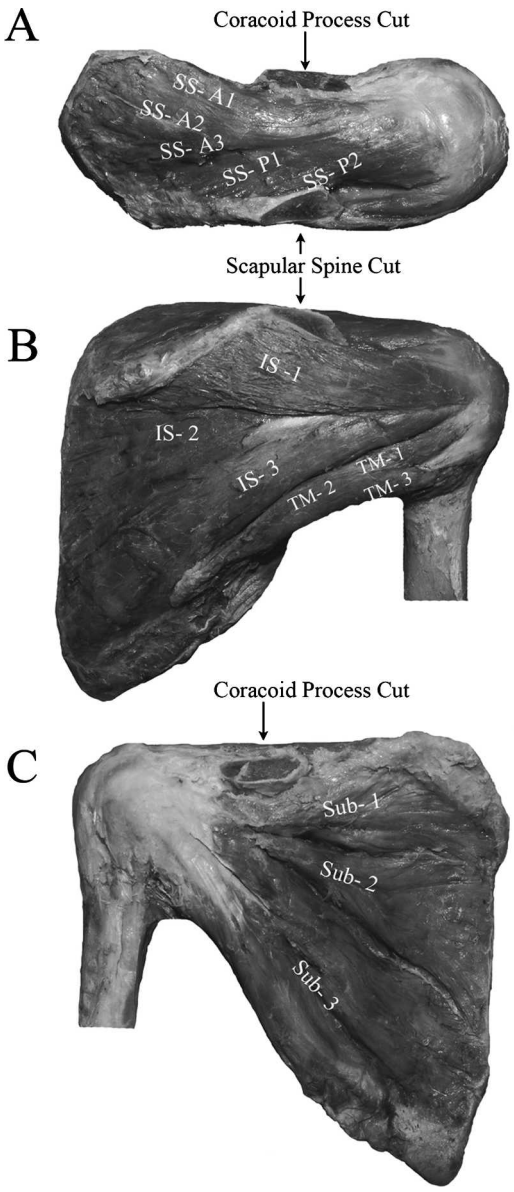

Fig 1A–C. The photographs show a right shoulder with the coracoid process and scapular spine cut to expose the (A) supraspinatus (SS), (B) infraspinatus (IS) and teres minor (TM), and (C) subscapularis (Sub). The supraspinatus was divided into five regions: A1–3 in the anterior belly and P1–2 in the posterior belly. The infraspinatus, teres minor, and subscapularis were divided into three regions corresponding to superior, middle, and inferior regions.

functions were adapted from published data[21] to define muscle length change as a function of joint angle. Muscle fiber lengths and serial sarcomere numbers were scaled to match a 51-mm humeral head.[21] The length changes were distributed evenly among the sarcomeres in each muscle fiber. Active and passive tension values were computed using length-tension curves derived from human muscle.[18,19] Using the computed tension values, sarcomere lengths were iteratively adjusted for tendon strain.[18] To understand the behavior of the operating range-joint angle and relative tension-joint angle profiles, the glenohumeral joint was modeled in all permutations of 75° medial and lateral rotation (internal and external rotation) to 75° abduction in the scapular plane. This yielded the sarcomere length-joint angle and active and passive-tension surfaces.

Rotator cuff muscle comparisons were made with one-way repeated analyses of variance (ANOVA) after confirming the assumptions of normality and homogeneity of variances. Post hoc t-tests with Bonferroni corrections were used to identify differences when main effects were identified. After the initial whole-muscle comparisons, within-muscle comparisons were made using one-way repeated ANOVA measures and post hoc t tests to identify regional fiber length differences. These comparisons determined the relative homogeneity of muscle fiber length in a muscle, and also determined the shape of the muscle length tension curve. The scaling functions (and confidence intervals) between muscle fiber length and humeral head diameter were computed using simple linear regression. Because the modeled operating range and relative tension-joint angle data represented mean values, between-muscle comparisons were not illustrated with statistical comparisons. All values are reported as mean ± standard error (SE) unless otherwise noted. Statistical tests were performed using SPSS software (SPSS, Inc, Version 11.5, Chicago, IL). Significance was set at the $p < 0.05$ level except for post hoc tests where $p < 0.05$ was adjusted according to the Bonferroni correction.

RESULTS

Muscle mass, muscle length, fiber length, and PCSA varied considerably. There were differences ($p < 0.05$) in muscle mass, with the subscapularis and infraspinatus as the heaviest and the longest (Table 1). Muscle fiber lengths were shortest ($p < 0.05$) in the supraspinatus. The L_f/L_m ratios were relatively small, but the subscapularis had the smallest ratio (Table 1). The supraspinatus and infraspinatus had longer ($p < 0.05$) resting sarcomere lengths than the teres minor and subscapularis (Table 1). The ratio of fiber length to sarcomere length was the serial sarcomere number (S_n), which was smallest ($p < 0.05$) in the supraspinatus (Table 1). The PCSA was different ($p < 0.05$) in all muscles, with the subscapularis having the largest and teres minor having the smallest PCSA (Table 1).

Muscle fiber length variability indicated regional differences were within 20%, except for the superior and inferior regions of subscapularis where they were within 27% (Fig 2). The superior and middle regions of infraspinatus also differed ($p < 0.05$). In general, across all muscles, inferior fibers tended to be longer than the superior fibers, and anterior fibers tended to be longer compared with posterior fibers.

Muscle fiber lengths scaled with humeral head diameter only in the supraspinatus and teres minor muscles (Table

TABLE 1. Muscle Architectural Properties*

Muscle	Mass (g)	Muscle Length (cm)	L_f (cm)	L_f/L_m	L_s (μm)	S_n	Pennation Angle (degrees)	PCSA (cm^2)
Supraspinatus	34.0 ± 4.3¶	8.5 ± 0.4¶	4.50 ± 0.32¶	0.53 ± 0.03‖	3.23 ± 0.05§,‖	16,655 ± 1182¶	5.1 ± 0.8¶	6.65 ± 0.56¶
Infraspinatus	78 ± 7.5¶	12.1 ± 0.5†,§	6.57 ± 0.33†	0.55 ± 0.02‖	3.18 ± 0.06§,‖	24,332 ± 1203†	1.4 ± 0.4†,‖	10.71 ± 0.95¶
Teres minor	21.2 ± 2¶	10.8 ± 0.6†,‡	6.09 ± 0.35†	0.57 ± 0.03‖	2.80 ± 0.07†,‡	22,569 ± 1299†	0.6 ± 0.3†	3.18 ± 0.30¶
Subscapularis	101.8 ± 11.5¶	13 ± 0.6†	6 ± 0.47†	0.45 ± 0.02¶	2.52 ± 0.09†,‡	22,069 ± 1735†	0 ± 0†,‡	15.53 ± 1.41¶

*Values are mean ± standard error of 10 specimens; †significantly different than supraspinatus; ‡significantly different than infraspinatus; §significantly different than teres minor; ‖significantly different than subscapularis; ¶significantly different than all other muscles; L_f = normalized fiber length; L_f/L_m = normalized fiber length/muscle length ratio; L_s = resting sarcomere length; S_n = sarcomere number; PCSA = physiologic cross-sectional area

2). However, none of the scaling functions had a slope near one, suggesting fiber length and skeletal dimensions may not increase proportionately.

The modeled operating ranges revealed the supraspinatus sarcomere lengths were most sensitive to abduction motions, whereas the infraspinatus, teres minor, and subscapularis were most sensitive to medial-lateral rotation motions (Supplemental material [Supplemental Fig 1] is available via the Article Plus feature at www.corronline.com.). The subscapularis operated over the widest range of sarcomere lengths (1.23–3.75 μm), followed by the infraspinatus (1.95–4.17 μm), teres minor (1.86–3.85 μm), and supraspinatus (1.95–3.39 μm). Despite these differences, muscles had sarcomere lengths between 1.5 μm and 3.25 μm (> 75% of maximum force generating capacity) throughout 72% (range, 68–80%) of the range of motion (ROM), and operated on the plateau of the length-tension curve throughout 10% (range, 9.8–11%) of the ROM (Supplemental material [Supplemental Fig 2] is available via the Article Plus feature at www.corronline.com). The passive tension distributions were more localized than the broad, active tension surfaces (Supplemental material [Supplemental Fig 2] is available via the Article Plus feature at www.corronline.com). Each muscle had a distinct region of passive tension production. For example, the subscapularis produced maximum passive tension in lateral rotation, whereas the infraspinatus produced maximum passive tension in internal rotation.

The subscapularis contributed 43% (range, 23–60%) of the total active tension, the infraspinatus contributed 28% (range, 0–44%), the supraspinatus contributed 21% (range, 14–44%), and the teres minor contributed 8% (range, 5–11%) (Supplemental materials [Supplemental Fig 3] is available via the Article Plus feature at www.corronline.com). The peak of the active tension surface was at 25º abduction and 20º lateral rotation. The supraspinatus and infraspinatus contributed 39% and 57%, respectively, of the total resting passive tension in the anatomic position, whereas the subscapularis contributed 100% of the total

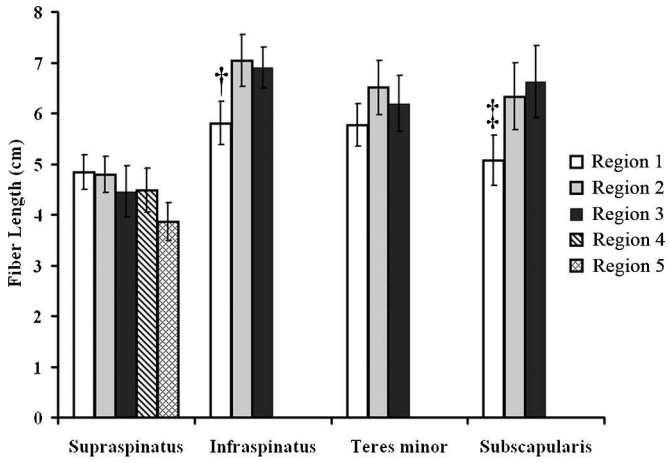

Fig 2. A graph shows muscle fiber length in different regions of the rotator cuff. Regions 1–3 refer to SS–A1 through SS–A3 and Regions 1–3 in all other muscles, whereas Regions 4 and 5 refer to SS–P1 and SS–P2. Muscle fiber lengths in the superior regions (Region 1) of the infraspinatus and subscapularis were shorter than more inferior regions (Region 3) of the same muscles. The bars indicate mean ± standard deviation from 10 independent specimens (†the superior region of the infraspinatus had shorter ($p = 0.006$) muscle fiber lengths than the middle region; ‡the superior region of subscapularis muscle had shorter ($p = 0.029$) muscle fiber lengths than the inferior region).

TABLE 2. Scaling Relations for Normalized Muscle Fiber Length (cm) as a Function of Anatomic Neck Diameter (cm)

Muscle	Slope	Y Intercept	r^2
Supraspinatus	1.94 ± 0.67	−4.06 ± 2.96	0.513*
Infraspinatus	1.42 ± 0.84	0.32 ± 3.67	0.265
Teres minor	2.27 ± 0.68	−3.93 ± 3.01	0.583*
Subscapularis	1.75 ± 1.26	−1.78 ± 5.58	0.195

*Significant regression model fit; values are mean ± standard deviation of 10 specimens

TABLE 3. Previous Architectural Studies*

	Roh et al[26] (2000) (n = 25)		Bassett et al[3] (1990) (n = 4; 3 bilateral)		Aluisio et al[2] (2003) (n = 5)	
Muscle	*Fiber length (cm)*	*PCSA (cm^2)*	*Fiber length (cm)*	*PCSA (cm^2)*	*Fiber length (cm)*	*PCSA (cm^2)*
Supraspinatus	7.44 ± 1.04	2.02 ± 0.35	6.95 ± 0.07	5.7 ± 1.2	6.06 ± 0.32	5.26 ± 0.71
Infraspinatus	—	—	8.9 ± 0.57	13.7 ± 3.9	7.98 ± 0.64	9.94 ± 2.01
Teres minor	—	—	—	—	6.78 ± 0.61	2.36 ± 0.56
Subscapularis	—	—	8.05 ± 0.92	16.3 ± 7	6.80 ± 0.54	15.6 ± 2.31

*Values are mean ± standard error; no parameters are normalized to sarcomere length; PSCA = physiologic cross-sectional area

passive tension at maximum abduction and lateral rotation (Supplemental material [Supplemental Fig 4] is available via the Article Plus feature at www.corronline.com). Passive tension was relatively low in abduction and lateral rotation.

DISCUSSION

We defined the architectural properties of the rotator cuff muscles and predicted their operating ranges by performing detailed architectural measurements and calculations on fixed human tissue. We then created a simple lumped parameter model to estimate the sarcomere length-joint angle and relative tension-joint angle relationships for each muscle and the rotator cuff.

Our study has several limitations. First, formalin fixation shrinks tissue approximately 10%,[6] which means our normalized fiber-length data and the initial sarcomere lengths may have been underestimated. However, normalized fiber length would be unaffected. Second, the muscle excursion functions were regression-based, meaning there is some inherent uncertainty in how well the predicted excursions match individual data. Regional sarcomere length differences were not considered, such as those possibly occurring when only a portion of a muscle is stretched over a bony prominence. Third, there were no in vivo data available to calibrate our sarcomere length-joint angle results. Finally, fixation position was an estimate of the neutral joint configuration and may not reflect the clinically accepted definition of 0º abduction, flexion, and lateral rotation. However, the purpose of this model was to gain an understanding of the relative changes in the sarcomere length and relative tension as a function of joint angle. The modeled data were within the physiologic range of sarcomere lengths, which provides confidence in our scaling and modeling algorithms. The most important future experiment to calibrate the model would be to measure in situ passive length-tension and sarcomere length-joint angle relationships. To make the model most useful, accurate muscle excursion-joint angle relationships are needed for all three planes of motion.

Our supraspinatus and infraspinatus muscle fiber lengths were approximately 20% shorter, and our PCSAs were approximately 20% larger than reported by Alusio et al (Tables 1, 3).[2] These differences are explained primarily by our sarcomere length normalization procedures. Supraspinatus and infraspinatus-measured sarcomere lengths were 3.23 μm and 3.18 μm, respectively, longer than the optimal sarcomere length of 2.7 μm. Therefore, normalizing these fiber lengths would shorten the overall muscle fiber lengths, increasing PCSA by approximately 15% (Table 3).

The rotator cuff muscles are capable of producing relatively large forces compared with the biceps, brachialis, brachioradialis, and posterior deltoid, yet they have smaller excursions compared with many of the digital and elbow flexors and extensors (Fig 3).[7,15] The architectural arrangement of the rotator cuff muscle fibers indicates they are designed for force production rather than excur-

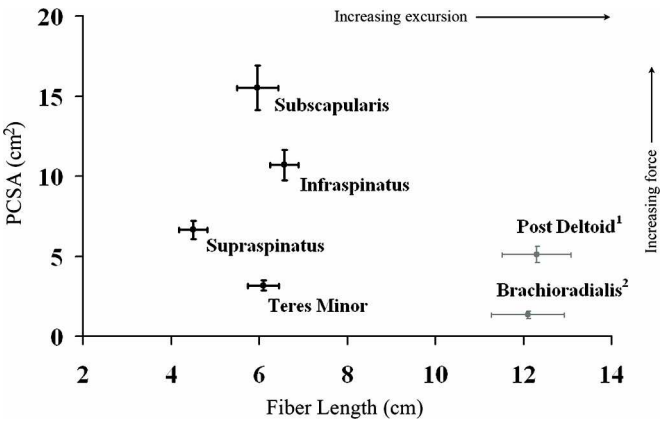

Fig 3. A scatter plot shows muscle fiber length (abscissa) versus physiologic cross-sectional area (ordinate). The subscapularis produced the largest forces, and the supraspinatus muscle had the shortest excursion range. Values are mean ± standard error for 10 specimens. The short fiber lengths and large PCSAs of the rotator cuff muscles compared with other muscles in the upper extremity (posterior deltoid and brachioradialis muscles) indicate their stabilizing function. [1]Data from Friden et al[7]; [2]Data from Lieber et al[17]

sion, which is consistent with their proposed role of stabilizing the humeral head in the glenoid. Because of the limited stabilization afforded by the shallow glenoid and the variety of shoulder positions, it seems intuitive the joint would require robust yet adaptable soft tissue stabilization over a range of joint positions. The modeled sarcomere length-joint angle and relative tension-joint angle relationships support this proposed functional role, as all muscles generated relatively large tensions over most joint angles.

Based on architecture alone, the short and relatively homogeneous fiber lengths of these muscles imply they would function efficiently over a relatively narrow range of sarcomere lengths. However, the modeled sarcomere length operating ranges indicate resting sarcomere lengths, fiber lengths, and moment arms are all tightly regulated, allowing the rotator cuff muscles to produce near-maximal active tensions in midrange and produce passive tensions at rest and in extreme joint positions. However, the combination of short fibers and long resting sarcomere lengths make this muscle relatively sensitive to stretch so small perturbations would result in relatively high restoring forces.[22,23,30] Therefore, for muscles with similar pennation angles but with differing fiber lengths, imposing a given stretch across the muscle will lengthen each sarcomere in a short fiber to a greater extent compared with those in a long fiber. Contractile function may be compromised if the muscle is moved to the descending limb of its length-tension curve (eg, if sarcomeres are stretched so myofilament overlap is critically decreased).[12]

Our findings have important implications for current strategies of rotator cuff repair. During traditional repairs, the retracted muscle and tendon often are mobilized and stretched to permit reattachment as close to the original insertion site as possible. This is based on the assumption that stretching the musculotendinous unit to its original length restores normal anatomy and native function. In the acute setting, this may restore optimal gross and ultrastructural muscle length if the musculotendinous length is maintained and extensive débridement is not necessary. However, this technique may be detrimental to muscle function in the common condition of retraction and reorganization as observed in chronic tears. Chronic rotator cuff tears are commonly associated with changes including fatty infiltration, net loss of muscle volume, and extensive retraction.[14,32] These changes may accompany remodeling in the muscle by subtraction of serial sarcomeres, as has been reported after tenotomy in other systems.[1] Hypothetically, the sensitivity of the supraspinatus to stretch would be compounded in a chronically retracted muscle with sarcomere subtraction. If the repair required muscle advancement, then one reasonably could expect the sarcomere length-joint angle and relative tension-joint angle curves to shift to very long lengths, resulting in profound muscle weakness.

Our data suggest the rotator cuff muscles collectively reach their optimum force-producing capacity at approximately 25º abduction and 20º lateral rotation. Our data also indicate passive joint stability in the anatomic position was due to the relatively long supraspinatus and infraspinatus resting sarcomere lengths, whereas stability in the position of instability (abduction and lateral rotation) was due to the subscapularis.

The sarcomere length operating-range data could be used to optimize rotator cuff strengthening programs. Newham et al[20] suggested eccentric-induced muscle injury and strengthening may be more pronounced when muscles are loaded at longer lengths. This implies muscle strengthening may be more efficacious at longer muscle lengths, assuming the patient is not placed in a position of impingement or instability.

In summary, the rotator cuff architecture suggests these muscles are designed primarily for force production, congruent with their role as shoulder stabilizers. The consistently short muscle fiber lengths suggest rotator cuff muscles (particularly the supraspinatus) are highly sensitive to length changes, and function after repair depends on the site of tendon anastomosis. Clinically, the implication is that relatively small changes to rotator cuff muscle length occurring during surgery may result in relatively large changes in shoulder function.

Acknowledgments

We thank James Esch, MD, for assistance in obtaining shoulder specimens and Michael Ryan, BS, for technical assistance.

References

1. Abrams RA, Tsai AM, Watson B, Jamali A, Lieber RL. Skeletal muscle recovery after tenotomy and 7-day delayed muscle length restoration. *Muscle Nerve*. 2000;23:707–714.
2. Aluisio FV, Osbahr DC, Speer KP. Analysis of rotator cuff muscles in adult human cadaveric specimens. *Am J Orthop*. 2003;32:124–129.
3. Bassett RW, Browne AO, Morrey BF, An KN. Glenohumeral muscle force and moment mechanics in a position of shoulder instability. *J Biomech*. 1990;23:405–415.
4. Bodine SC, Roy RR, Meadows DA, Zernicke RF, Sacks RD, Fournier M, Edgerton VR. Architectural, histochemical, and contractile characteristics of a unique biarticular muscle: the cat semitendinosus. *J Neurophysiol*. 1982;48:192–201.
5. Codman EA. The Classic: Rupture of the supraspinatus tendon. 1911. *Clin Orthop Relat Res.* 1990;254:3–26.
6. Eisenberg BR. Quantitative ultrastructure of mammalian skeletal muscle. In: Peachey LD, Adrian RH, eds. *Handbook of Physiology: Section 10: Skeletal Muscle.* Baltimore, MD: American Physiological Society; 1983:73–112.
7. Fridén J, Lieber RL. Quantitative evaluation of the posterior deltoid-to-triceps tendon transfer based on muscle architectural properties. *J Hand Surg Am*. 2001;26:147–155.
8. Fridén J, Lieber RL. Mechanical considerations in the design of surgical reconstructive procedures. *J Biomech*. 2002;35:1039–1045.

9. Fridén J, Lieber RL. Tendon transfer surgery: clinical implications of experimental studies. *Clin Orthop Relat Res.* 2002;403(Suppl): S163–S170.
10. Fuchs S, Chylarecki C, Langenbrinck A. Incidence and symptoms of clinically manifest rotator cuff lesions. *Int J Sports Med*. 1999; 20:201–205.
11. Gans C. Fiber architecture and muscle function. In: Teijung RT, ed. *Exercise and Sport Science Reviews*. Philadelphia, PA: Franklin University Press; 1982:160–207.
12. Gordon AM, Huxley AF, Julian FJ. The variation in isometric tension with sarcomere length in vertebrate muscle fibres. *J Physiol*. 1966;184:143–169.
13. Harryman DT II, Mack LA, Wang KY, Jackins SE, Richardson ML, Matsen FA III. Repairs of the rotator cuff: correlation of functional results with integrity of the cuff. *J Bone Joint Surg Am*. 1991;73: 982–989.
14. Kjeldsen SR, Tordrup PJ, Hvidt EP. Return to sport after a Bankart operation of the shoulder using the Mitek anchor system. *Scand J Med Sci Sports*. 1996;6:346–351.
15. Lieber RL, Fazeli BM, Botte MJ. Architecture of selected wrist flexor and extensor muscles. *J Hand Surg Am*. 1990;15:244–250.
16. Lieber RL, Fridén J. Functional and clinical significance of skeletal muscle architecture. *Muscle Nerve*. 2000;23:1647–1666.
17. Lieber RL, Jacobson MD, Fazeli BM, Abrams RA, Botte MJ. Architecture of selected muscles of the arm and forearm: anatomy and implications for tendon transfer. *J Hand Surg Am*. 1992;17:787–798.
18. Lieber RL, Loren GJ, Fridén J. In vivo measurement of human wrist extensor muscle sarcomere length changes. *J Neurophysiol*. 1994; 71:874–881.
19. Lieber RL, Murray W, Clark DL, Hentz VR, Fridén J. Biomechanical properties of the brachioradialis muscle: implications for surgical tendon transfer. *J Hand Surg Am*. 2005;30:273–282.
20. Newham DJ, Jones DA, Ghosh G, Aurora P. Muscle fatigue and pain after eccentric contractions at long and short length. *Clin Sci*. 1988;74:553–557. [Lond]
21. Otis JC, Jiang CC, Wickiewicz TL, Peterson MG, Warren RF, Santner TJ. Changes in the moment arms of the rotator cuff and deltoid muscles with abduction and rotation. *J Bone Joint Surg Am*. 1994; 76:667–676.
22. Petit J, Filippi GM, Emonet-Dénand F, Hunt CC, Laporte Y. Changes in muscle stiffness produced by motor units of different types in peroneus longus muscles of cat. *J Neurophysiol*. 1990;63: 190–197.
23. Petit J, Filippi GM, Gioux M, Hunt CC, Laporte Y. Effects of tetanic contraction of motor units of similar type on the initial stiffness to ramp stretch of the cat peroneus longus muscle. *J Neurophysiol*. 1990;64:1724–1732.
24. Post M, Silver R, Singh M. Rotator cuff tear: diagnosis and treatment. *Clin Orthop Relat Res.* 1983;173:78–91.
25. Powell PL, Roy RR, Kanim P, Bello M, Edgerton VR. Predictability of skeletal muscle tension from architectural determinations in guinea pig hindlimbs. *J Appl Physiol*. 1984;57:1715–1721.
26. Roh MS, Wang VM, April EW, Pollock RG, Bigliani LU, Flatow EL. Anterior and posterior musculotendinous anatomy of the supraspinatus. *J Shoulder Elbow Surg*. 2000;9:436–440.
27. Sacks RD, Roy RR. Architecture of the hindlimb muscles of cats: functional significance. *J Morphol*. 1982;173:185–195.
28. Vahlensieck M. an Haack K, Schmidt HM. Two portions of the supraspinatus muscle: a new finding about the muscles macroscopy by dissection and magnetic resonance imaging. *Surg Radiol Anat*. 1994;16:101–104.
29. Vahlensieck M, Pollack M, Lang P, Grampp S, Genant HK. Two segments of the supraspinous muscle: cause of high signal intensity at MR imaging? *Radiology*. 1993;186:449–454.
30. Walmsley B, Proske U. Comparison of stiffness of soleus and medial gastrocnemius muscles in cats. *J Neurophysiol*. 1981;46:250–259.
31. Ward SR, Lieber RL. Density and hydration of fresh and fixed human skeletal muscle. *J Biomech*. 2005;38:2317–2320.
32. Williams GR Jr, Iannotti JP, Rosenthal A, Kneeland JB, Dalinka M, Schwaam H. Anatomic, histologic, and magnetic resonance imaging abnormalities of the shoulder. *Clin Orthop Relat Res.* 1996;330: 66–74.

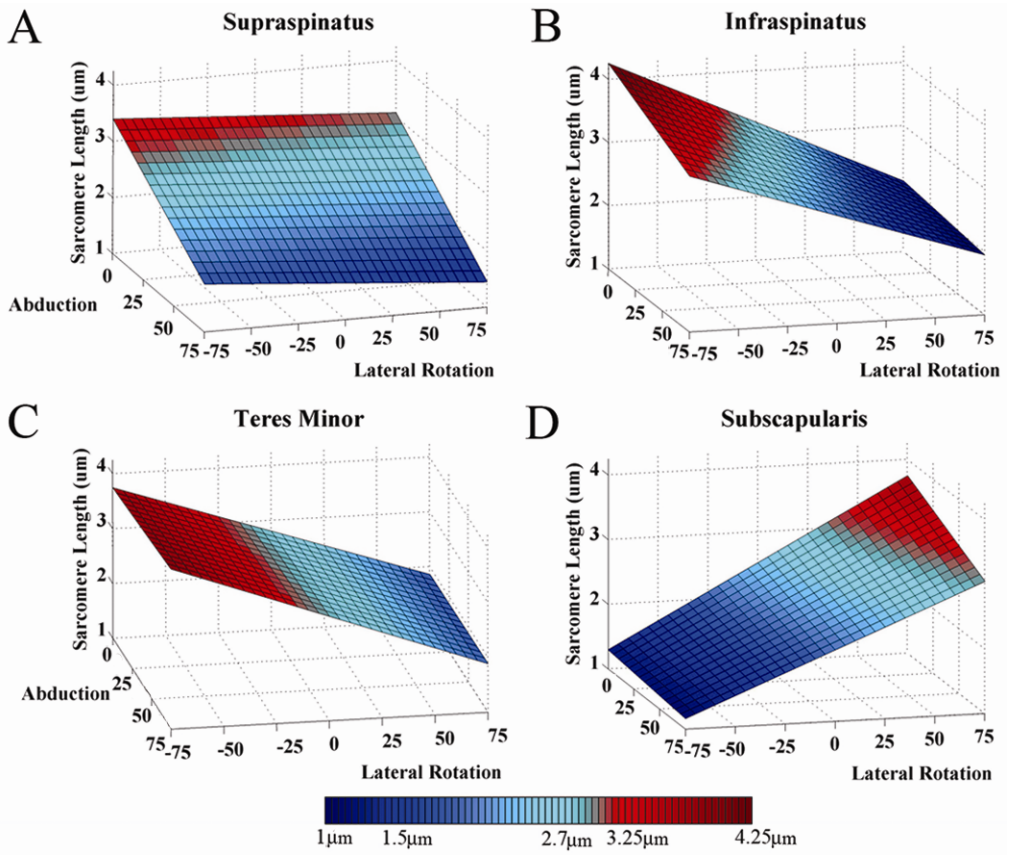

Supplemental Fig 1A–D. Graphs show the sarcomere length operating ranges of the (A) supraspinatus, (B) infraspinatus, (C) teres minor, and (D) subscapularis as a function of abduction (x axis) and medial-lateral rotation (y axis). All muscles operated within the physiological range of sarcomere lengths, but the supraspinatus was most sensitive to changes in abduction angle. The other muscles were more sensitive to medial-lateral rotation. As expected, the subscapularis was the only muscle that lengthened during abduction and lateral rotation.

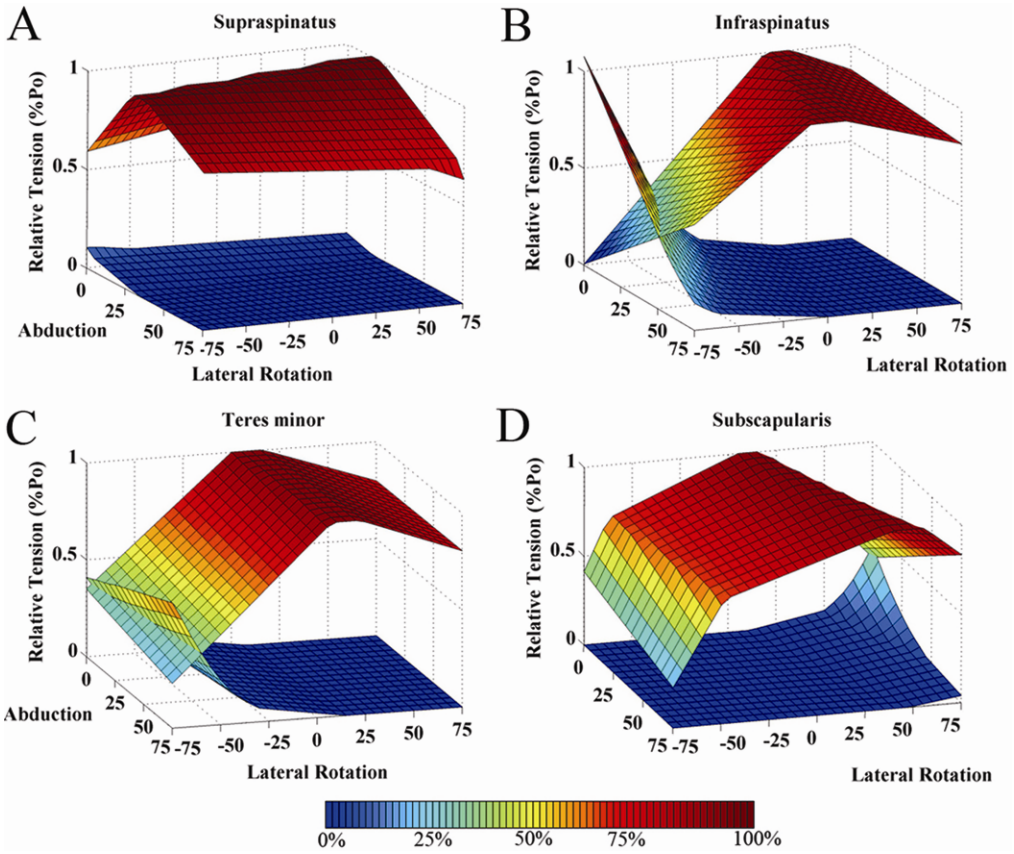

Supplemental Fig 2A–D. Graphs show the active (upper surface) and passive (lower surface) relative tension profiles of the (A) supraspinatus, (B) infraspinatus, (C) teres minor, and (D) subscapularis muscles as a function of abduction (x axis) and medial-lateral rotation (y axis). Muscles were able to generate at least 75% of their maximum active tension through the majority of ranges of motion, while passive tension peaked in specific joint configurations for each muscle.

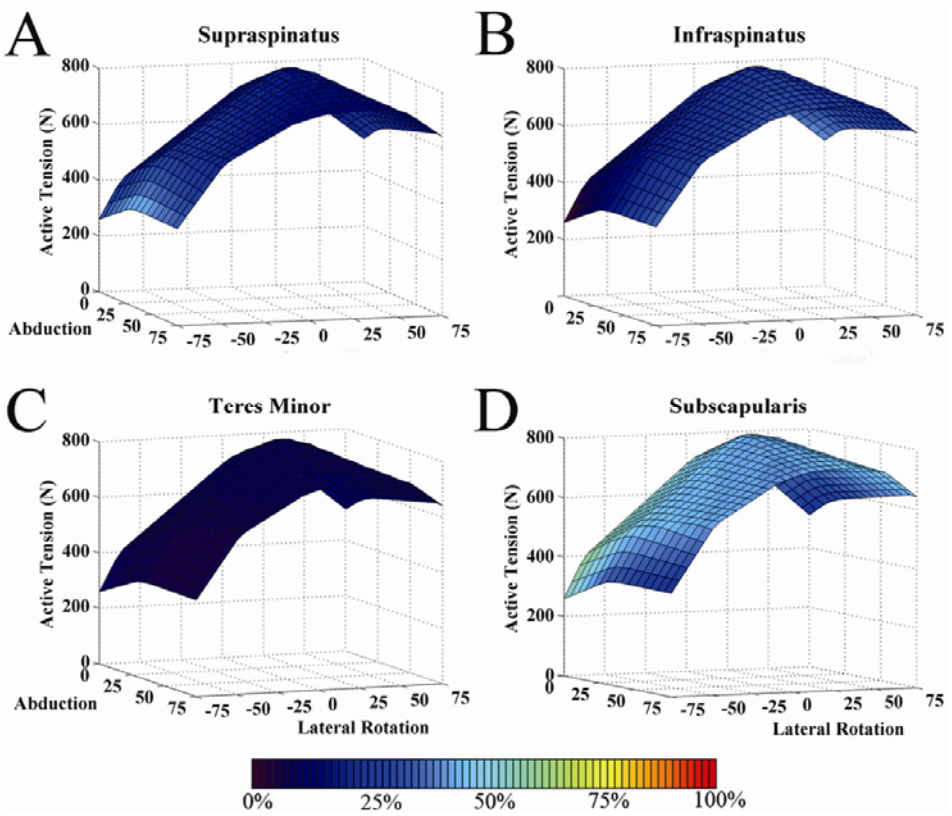

Supplemental Fig 3A–D. Graphs show the percent contributions to the total active tension profile for (A) supraspinatus, (B) infraspinatus, (C) teres minor, and (D) subscapularis muscles as a function of abduction (x axis) and medial-lateral rotation (y axis). The total active tension surface peaks at 25º of abduction and 20º of lateral rotation. The subscapularis makes the largest contribution to total active tension followed by the infraspinatus, supraspinatus, and teres minor.

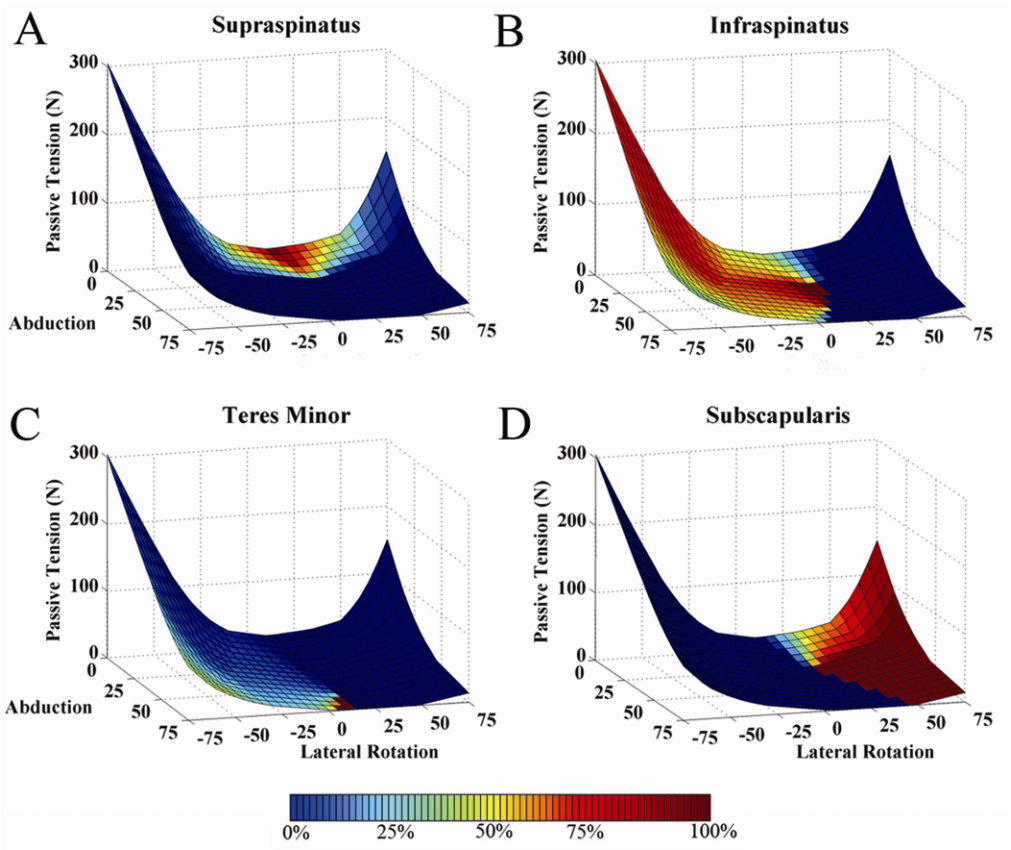

Supplemental Fig 4A–D. Graphs show the percent contributions to the total passive tension profile for the (A) supraspinatus, (B) infraspinatus, (C) teres minor, and (D) subscapularis muscles as a function of abduction (x axis) and medial-lateral rotation (y axis). The total passive tension surface peaks in maximum medial and lateral rotation. The supraspinatus and infraspinatus contribute 39% and 57%, respectively, to the total passive tension at rest (anatomical position). The subscapularis supports 100% of the passive tension load in maximum abduction and lateral rotation.